LA-UR-98-1523

Approved for public release; distribution is unlimited.

Title: DYNAMICS OF QUANTUM WAVE PACKETS

Author(s): Timothy R. Gosnell, MST-10

Antoinette J. Taylor, George Rodriguez, Tracy S. Clement, MST-11

Submitted to: DOE Office of Scientific and Technical Information (OSTI)

Los Alamos
NATIONAL LABORATORY

DISCLAIMER

DISCLAIMER

Portions of this document may be illegible in electronic image products. Images are produced from the best available original document.

Dynamics of Quantum Wave Packets

Timothy R. Gosnell* (MST-10), Antoinette J. Taylor (MST-11),
George Rodriguez (MST-11), and Tracy S. Clement (MST-11)

Abstract

This is the final report of a three-year, Laboratory Directed Research and Development (LDRD) project at the Los Alamos National Laboratory (LANL). The objective of this project was to develop ultrafast laser techniques for the creation and measurement of quantum vibrational wave packets in gas phase diatomic molecules. Moreover, we sought to manipulate the constitution of these wave packets in terms of harmonic-oscillator basis wavefunctions by manipulating the time-dependent amplitude and phase of the incident ultrashort laser pulse. We specifically investigated gaseous diatomic potassium (K_2), and discovered variations in the shape of the wave packets as a result of changing the linear "chirp" in the ultrashort preparation pulse. In particular, we found evidence for wave-packet compression for a specific degree of chirp. Important ancillary results include development of new techniques for denoising and deconvolution of femtosecond time traces and techniques for diagnosing the phase and amplitude of the electric field of femtosecond laser pulses.

Background and Research Objectives

Pick an atom out of a box, and ask about its quantum state. The most natural response for most of us—perhaps after performing a measurement—would be something like, "The atom is in its third excited state," or "The atom is in its ground state." The point is that quantum states of atoms and molecules are almost universally viewed in terms of their respective *energy* eigenfunctions; yet the superposition principle tells us that an infinite number of solutions to the Schrödinger equation can be constructed at will from eigenstates drawn from any given complete set of mutually commuting operators. For example, a perfectly valid solution to the quantum equations of motion for the harmonic oscillator might be a sum in equal proportions of the first, third, and sixth harmonic-oscillator eigenfunctions. A more subtle aspect of this superposition is the explicit quantum-phase relationships that might exist between these constituent eigenfunctions.

This project concerns the controlled assembly of such quantum-mechanical wave packets in simple molecular systems. Of special interest is their subsequent dynamical evolution. With carefully tailored femtosecond laser pulses, we will demonstrate the

* Principal Investigator, email: gosnell@lanl.gov

construction of quantum states of matter otherwise not available in nature and ask how the exact details of the superposition process uniquely affect dynamical histories. The larger scientific issues underpinned by this research are how atomic and molecular "designer" dynamics might be applied in fundamental studies of small quantum systems, and how they might be exploited in real technological applications.

Experimental design in femtosecond molecular physics has been dominated by the crudest characteristics of ultrashort optical pulses, namely, their time duration and intensity amplitudes. Corkum was among the first to emphasize that the details of optical phase offered a wealth of opportunities in the development of new experimental concepts for the study of ultrafast physical phenomena. An early experiment motivated by this thinking was the observation of population interference effects in optically excited I_2 that resulted from adjustable interpulse delays of two phase-locked ultrashort pulses. In further theoretical work, Brumer and Shapiro showed how phase-coherent optical excitation of molecules could create quantum interference effects in nuclear wave functions that directly affected the outcome of dissociation reactions. But the subject of coherent control of wave-packet dynamics experienced its first major advance when Kosloff *et al.* borrowed optimal-control algorithms more familiar to systems engineers and applied them to molecular quantum dynamics. As shown by these workers, the optimization problem consists of giving a general prescription for the temporal shape, overall intensity, and phase history for an optical field that controls the outcome of a molecular dynamical process. Included among the input data is precise knowledge of transition oscillator strengths, bound-state electronic and vibrational energies, and internuclear potential-energy hypersurfaces. This work has spawned a major cottage industry within theoretical chemical physics, and has even advanced to the point where genetic learning algorithms have been designed into model experiments so that the completeness and specificity of the required input data can be relaxed.

Experimental investigations in wave-packet dynamics on molecular potential energy surfaces has not kept pace with the substantial theoretical progress just described. The reasons are the practical difficulties connected with shaping and diagnosing the intensity and phase profiles of a femtosecond pulse. In the two years prior to the beginning of this project, our efforts to develop intensity and phase-sensitive pulse diagnostic techniques had matured to the point where meaningful experiments in wave-packet dynamics could be attempted. We intended to develop two specific types of experiments. In the first, wave packets prepared with a variety of chirp- and amplitude-controlled pulse sequences were to be assembled on the bound excited-state potential surface of gas-phase Cs_2 or K_2 molecule and the photoionization rate from this state would be measured as a function of time. The ionization data would then expose interference effects between eigenfunction components of the wave packet, as well as

the rate of wave-packet dephasing resulting from the molecule-dependent energy-momentum dispersion relation for particles moving on the chosen potential surface. In the second experiment, an iterative procedure would be used to build a "molecular cannon" wave packet on a repulsive potential surface of gas-phase I_2. The idea here is that as a properly assembled wave packet slides down the repulsive surface, the packet will at some point along its trajectory coalesce to some minimum spatial width detectable as a femtosecond blip in a pump-probe laser-induced fluorescence measurement.

Research in wave-packet dynamics is in its infancy. It is not yet known how sensitive the control field will be to uncertainties in our knowledge of potential energy surfaces; nor is it known whether simple approximations to complicated control fields will be good enough to achieve desired effects; nor is it known if there is a limit to the specificity of a molecular process if only parts of the dynamics are controlled from outside. Our experiments will begin to address these questions.

Importance to LANL's Science and Technology Base and National R&D Needs

Optical-pulse-shaping technology and diagnostics are of special relevance to Laboratory weapons programs that rely on short-pulse lasers. These include Above Ground Experimentation (AGEX), Inertial Confinement Fusion (ICF), and potential nonlethal defense programs.

A research program in ultrafast ignitor concepts for laser fusion has begun at Livermore and LANL. This new approach achieves target ignition with a high-intensity picosecond laser pulse rather than by hydrodynamic compression, hence eliminating much of the drive energy needed by the ignition process. Fast ignitor systems could therefore significantly reduce the cost of the National Ignition Facility, a laser fusion project founded on a new 800-million-dollar glass laser currently under design. Special shaping of a picosecond ignition pulse may further enhance either its ability to ignite the fuel or its ability to propagate through a long-scale-length plasma to the interaction region of the target. The short ignition pulse for such a system would be produced by chirped-pulse amplification in a high-energy glass laser; hence techniques for pulse formation and diagnosis developed in this project are directly applicable to fast-ignitor technology.

Short-pulse laser-interaction physics is one of several AGEX programs at LANL. In earlier experiments, the Los Alamos Bright Source was used to produce extremely high electron temperatures, x-ray fluxes, and shock amplitudes in solid targets. Current research on the Trident laser system is partially devoted to these same objectives. Pulse-shaping concepts have yet to be applied to these problems yet present a wealth of potential flexibility in the design of high-energy-density experiments applicable to the understanding of weapons

physics. Just one example of an experiment of special interest is the comparison of efficiencies for keV x-ray generation from solid targets exposed either to a single laser pulse or to a shaped pulse or pulse train.

Finally, pulse-shaping techniques can be used to produce a series of tailored optical pulses whose duration and spacing affect the resonant excitation of coherent plasma oscillations. Such oscillations emit high-intensity terahertz radiation from the plasma target, radiation that is capable of disrupting electronic devices from remote locations. Such sources are therefore of special interest to the DoD nonlethal defense community.

Scientific Approach and Accomplishments

An existing pump-probe apparatus based on an ultrafast Ti: sapphire laser was used both to produce quantum wave packets in diatomic molecules and to interrogate their dynamics. At the beginning of the project, the laser system had been fully operational for nearly a year and currently produces 50-mJ, 125-fs pulses tunable in the near infrared around 760-840 nm. Additional wavelengths have been obtained from the system by using nonlinear frequency-mixing techniques. A unique diagnostic, developed at Los Alamos, was adapted to our quantum dynamics application and used to fully characterize the electric-field amplitude and phase of output pulses produced by the Ti:sapphire system and its appended pulse-shaping optics.[1]

Our first task was to generate and detect quantum wave packets in K_2. An experimental apparatus for this purpose was designed, built, and tested; a schematic diagram of this apparatus is shown in Figure 1. Referring to the figure, the apparatus functions in the following way.

First, the 830-nm output of the amplified Ti:sapphire laser is split into two pieces. The first of these is propagated through an optical delay line after which it is injected into a heat pipe containing K_2 gas. The heat pipe is also fitted with electrodes for collection of electric charges produced in the cell and driven by a high voltage bias applied to the electrodes; the purpose of this configuration will be made clear below. The purpose of the pump pulse is to excite K_2 from its electronic ground state to an excited electronic state energetically matched to the pump photon energy. Since the equilibrium internuclear separation is different in the newly created excited state, the molecule begins to vibrate at a frequency determined by the internuclear potential energy.

The second pulse is focused into a liquid water cell where the pulse is converted into a broad-band "continuum" whose spectrum covers the range from 400 to 500 nm but whose time duration is still 120 fs. When combined with narrow band pass filters, this probe pulse effectively becomes a tunable source for interrogating the state of the excited gas as a function

of the time delay between the pump and the probe. Ultimately, two-photon ionization of the K_2 gas as a consequence of absorption of both a pump *and* a probe photon yields an ionization signal that is synchronously detected with a lock-in amplifier referenced to an optical chopper placed in either the pump or the probe beam. (The repetition rate of the amplified Ti:sapphire laser is 1 KHz, which permits optical chopping in the several-hundred-Hz range.) By virtue of the time delay between the ultrashort pump and probe pulses, the ionization signal gives information on the relative positions of the two K nuclei, or in quantum language the position and shape of the vibrational wave packet.

Figure 2 shows the ionization signal observed as a function of the delay time between the pump and the probe for a series of four probe wavelengths. As seen in the figure, little evidence is observed at a probe wavelength of 480 nm for creation and oscillation of vibrational wave packets in the K_2 molecule, while clear oscillations are observed at a wavelength of 415 nm. In order to confirm that these oscillations are indeed quantum wave packets affiliated with vibrational motion of the molecule, a Fourier transform of the data in Figure 2 (d) was performed; the result is shown in Figure 3. The spectral peak at 1.953 THz corresponds exactly with the known vibrational frequency of K_2 in the specific electronic excited state prepared by the pump pulse. The additional peak at 3.906 THz is the second harmonic of the fundamental vibration frequency; its presence in the spectrum represents the expected non-sinusoidal shape of the wave packet.

Close inspection of Figure 2(d), however, indicates the possibility that rather than a simple recurrence of a single compact wave packet, a double-peaked structure is observed on each recurrence of the packet. To test the theoretical validity of this possibility, a semiclassical calculation of the expected ion signal based on density-matrix was carried out and compared with the data. The result is shown in Figure 4, in which the data of Figure 2 (d) and the calculated theoretical signal are superimposed. While good agreement is obtained for the times of recurrence of the wave packet, and qualitative evidence is available for a double-peaked structure in the first recurrence or two of the wave packet, the signal-to-noise ratio proved inadequate to the task of experimentally demonstrating the persistent recurrence of the double-peaked wave packet structure.

Another question we asked of our simple theoretical model was whether it would reproduce the wavelength dependence of the signals shown in Figure 2. For this purpose, calculated time-resolved ionization signals for different probe wavelengths are shown in Figure 5. Respectable qualitative agreement is obtained, but the model fails to show the apparent monotonic increase in the amplitude of the oscillating wave packet. These results have been drafted in a manuscript to be submitted to *Chemical Physics Letters*.[2]

At this stage of the research, the following salient conclusions had been drawn:

- **Quantum wave packets in gas-phase K_2 had been definitively demonstrated.**
- **Improvements in signal-to-noise ratio would be necessary to advance the work toward the objective of observing pump-pulse-dependent wave packet shapes and dynamics.**
- **Better theoretical tools would be required to more quantitatively account for the data.**

Two separate activities were begun in pursuit of the second item above. A systematic investigation of noise sources in the experiment was instigated to speed data acquisition and minimize the influence of signal drifts. Of greater originality, a radical new approach to data processing was investigated and found useful for the analysis of time-resolved dynamics. Originally motivated by the need for better image processing algorithms in the astronomical community, this approach is finding increasing application in the astronomical arena but has yet to penetrate other scientific disciplines. Our efforts to develop and apply these new methods to the treatment of femtosecond spectroscopic data represented their first such application outside of astronomical imaging.

The task before us was to accomplish two independent objectives: remove random noise from the data to reveal the underlying "true" signal, and further to deconvolve the "true" signal from the inherent smearing effect of the finite probe-pulse width. The latter objective makes possible the discernment of finer detail in the signal not evident in the raw data; it is entails the perhaps surprising fact that an image can be made sharper than the fundamental diffraction limit would normally dictate. An indicator that the first of these tasks has been accomplished is to examine the arithmetic difference, or residuals, between the proposed or "hypothesis" signal and the data. If the residuals are indistinguishable from a series of random numbers distributed in accord with the known noise statistics of the measurements, then a valid hypothesis for the data has been found. All that would then be required would be to adopt a convention for which one of several equally valid hypotheses is to be chosen.

The second objective is far more difficult to accomplish. Were the data perfectly noiseless, then conventional Fourier-transform techniques could be applied to deconvolve the data from the point-spread function. The point spread function is the set of weights as a function of time over which the finite width of the probe pulse necessarily averages the instantaneous time-dependent signal—in the imaging analogy, the point spread function is the finite-width diffraction-limited spot created by a perfect point source when presented to the imaging system. In time-resolved data, a perfect zero-time-duration event would be smeared by the finite time width of the probe pulse, hence, the shape of the probe pulse is the point spread

function in this context. Fourier methods, although linear and computationally efficient, fail in deconvolving real data, however, because the input data are never noiseless and the Fourier transform is *extremely* noise sensitive.

Nonlinear methods have therefore been developed to accomplish both tasks of denoising and deconvolution. The most familiar of these are the so-called maximum entropy methods originally developed for analysis of radio-astronomy interferometric images. Although very effective, maximum entropy techniques suffer two crucial flaws: they often produce spurious signals where none exist and they often fail to yield residuals that are indistinguishable from random noise.

New methods free from these defects—known as pixon methods in the astronomical community—have been applied by us to simultaneously denoise and deconvolve time-resolved data, and further to select in a natural way a good hypothesis for the data from the multiple possibilities that are consistent with the data. The pixon method owes its heritage to maximum entropy and adaptive kernal smoothing algorithms. The method works roughly in the following way.

Imagine using a two-dimensional detector array to take a picture of some scene. Review of the captured image reveals random noise overlaid on the true image as one moves from pixel to pixel in the image. However, we note that many pixels appear to have the same amplitude as surrounding pixels and therefore might be averaged together to get a better value for the light amplitude in that region of the image. We can even imagine redesigning the camera with big detectors located where the original scene is either uniformly bright or particularly dim and small detectors where the scene is bright and highly structured. With the new camera, the image signal to noise would be greatly improved; in essence fewer degrees of freedom are available in the redesigned camera owing to the fewer detectors used in its construction. The fundamental advance offered by the pixon technique is that it provides a natural mechanism, based on statistical tests against the actual data of proposed true images, for algorithmically "redesigning the camera" and taking the picture again. The deconvolution portion of the problem is handled by simply taking a proposed true image, convolving it with the point spread function, and comparing it with the denoised data. A good match means a hypothesis image has been found, the algorithm selects a "good" hypothesis image by allowing no excess structure or detail to creep into the proposed true image—the detectors are not allowed to be smaller than is consistent with the data and the noise.

Figure 6 shows the application of pixon methods to data analogous to that of Figure 2 (d). Shown are both the raw data as captured straight from the lock-in amplifier and a hypothesis reconstruction derived from this data. This result shows the promise of pixon methods for analyzing data of this type, but it also illustrates that further development is needed

to avoid the obvious over resolution of the data appearing in the time window around 3 ps. This over resolution was most likely a result of the sparse data intrinsic to one-dimensional data sets—two-dimensional images offer a larger amount of data per unit length than one-dimensional data, implying that additional control in the pixon algorithm is required in the 1-D case. Nevertheless, the objective of denoising the data has been obtained at least in the time window between 0 and 2 ps. Closer inspection of the reconstruction also shows that higher resolution has been obtained as a consequence of successful deconvolution of the data from the point spread function. This result represents one of the major accomplishments of this project, one that will be generally applicable to all future femtosecond experiments and ultimately all experimental array data such as optical spectra, x-ray diffraction images, scanning tunneling microscope images, etc.

With these accomplishments in hand it became possible to attempt manipulating the shape of the detected wave packets by changing the characteristics of the pump pulse. A femtosecond laser pulse in its ideal state can be viewed as a superposition of "long" optical wave packets all with different frequencies. The term "long" here means that each packet must be long enough in time to be consistent with the spread of frequencies present in the packet but no longer. When all the packets are summed together with zero relative phase a much shorter burst of radiation is obtained. A pulse satisfying the condition of zero relative phase for its constituent wave packets is often called a transform-limited or zero-chirp pulse; it represents the shortest optical pulse possible consistent with the full frequency spectrum present in the pulse. If one were to take a snap shot of such a pulse it would look like a single sinusoid of well-defined frequency modulated by a gaussian-shaped amplitude function. As a sound wave it would sound like a "click." It was with a zero-chirp pump pulse that the data of Figure 2 and Figure 6 were taken.

By contrast, a positively chirped pulse is one with the same frequency content but with low-frequency constituent packets phase-shifted to earlier times and high-frequency packets phase-shifted to later times. The overall width of the pulse is now longer than in the transform-limited case; it would sound like a short whistled note sliding in pitch from low to high. Conversely, a negatively chirped pulse is constructed by phase shifting high frequency packets to earlier times and low-frequency packets to later times. Insofar as the optical pulse can be viewed as a superposition of long pulses with well defined frequencies, each optical wave packet can be viewed as establishing a narrow range of harmonic oscillator eigenfunctions in the excited electronic state of the molecule. Hence the relative timing of the constituent wave packets will have a profound impact on the relative phase of the full spectrum of harmonic oscillator eigenfunctions assembled in the harmonic internuclear potential of the excited electronic state.

Figures 7 and 8, in comparison with Figure 6, show the major accomplishment of this project. In Figure 7, a positively chirped pump pulse is used to excite the K_2 gas. The total energy and the frequency spectrum of this pump pulse are identical to that used to obtain the data in Figure 6. The data of the two figures show little difference, but for a possible enhanced asymmetry for the positively chirped pump pulse in the first and third returns of the wave packet.

Figure 8 shows the results of a negative chirp on the pump pulse. Again, the total energy and frequency spectrum of the pulse are identical to those used to acquire the data of Figures 6 and 7. The raw data and especially the hypothesis reconstruction exhibit "focusing" of the wave packet in the second recurrence at about t=1 ps. This focusing is a consequence of the slightly anharmonic potential the vibrational packets experience during oscillation; it has the effect of modifying the relative phase of the constituent harmonic-oscillator wave functions. For the negatively chirped pump pulse, this modification of the relative phase gives rise to a coherence in the second recurrence that compresses the probability density of the packet. In the case of the zero and positively chirped pulses, the initial conditions of relative phase established by the pump pulse are not properly arrayed so as to lead to wave packet compression in the second recurrence.

The main task remaining in this project is to quantitatively account for the data just discussed. We showed earlier that a simple model of the wave packet dynamics can qualitatively account for the packet shape but other features of the data are not predicted. To this end, we have been developing a new model of the wave packet optical interactions based on Liouville methods. This computational approach is essentially an extension of the semiclassical density-matrix methods we employed previously. It allows a more generalized picture of femtosecond optical interactions with matter and specifically makes natural the inclusion of finite temperature and rotational effects. Indeed it is the latter effects that most likely account for the overall decay of the vibrational wave packet amplitude with time. Upon completion of the theoretical analysis, the wave-packet compression results will be submitted for publication.[3]

The experiments discussed above represent some of the earliest attempts to create quantum states of matter not observable in conventional spectroscopic measurements or indeed in conventional ultrafast time-resolved measurements either. They illustrate the soundness of our premise that control over the quantum state of matter is possible. Since only the simplest of control techniques was investigated, i.e. the technique of simple linear frequency chirp imposed on the pump pulse, a wealth of additional experiments are possible to show further control over the wave packet. These include using both amplitude and frequency modulation in the pump pulse, multiple phase-locked pulses, and even pulse shaping of the probe pulse. The

next frontier for these types of experiments is possibly in condensed matter. We have already identified a condensed matter system that could show considerable simplification and much better signal properties than the gas system of the present project; the experiment is particularly attractive since experiments can be performed at cryogenic temperatures where wave packet coherence effects should be long lived.

Publications

1. Clement, T. S., Taylor, A. J., and Kane, D. J., "Single-Shot Measurement of the Amplitude and Phase of Ultrashort Pulses in the Violet," *Optics Lett.* **20**, 70-72 (1995).

2. Rodriguez, G., Taylor, A. J., and Gosnell, T. R., "Observation of K_2 Vibrational Wave Packets Between Similar Potential Surfaces," Los Alamos National Laboratory Report LAUR-96-1312.

3. Rodriguez, G., Taylor, A. J., and Gosnell, T. R., "Observation of Vibrational Wave Packet Focusing in Diatomic Potassium," in preparation.

Figure Captions

Figure 1. Experimental configuration used to detect vibrational quantum wave packets in K_2.

Figure 2. Time-resolved two-photon photoionization signals for gaseous K_2 at 800 K for four different probe wavelengths. The pump wavelength is 830 nm. The traces reveal the absence of wave packets for a detection wavelength of 480 nm and the gradual appearance of wave packet signatures as the wavelength of the probe is tuned towards 415 nm.

Figure 3. Fourier transform of the data shown in Figure 2. The peak at 1.953 THz corresponds exactly with the expected vibrational period of K_2 in the excited electronic state. The peak at the second harmonic demonstrates the essentially nonsinusoidal character of the photoionization signal.

Figure 4. Comparison of theory with experiment. The double-peaked structure of the recurring wave packet is predicted by a semiclassical density-matrix calculation, but the data does not offer sufficiently high signal to noise ratio to confirm agreement with theory at large time delays.

Figure 5. Additional theoretical calculations of the expected time-resolved photoionization signal as a function of the four probe wavelengths used to acquire the data of Figure 2. The appearance and disappearance of wave packet signatures between 480 and 440 nm is not observed in the experiment, suggesting that a more sophisticated model is required to quantitatively account for the data.

Figure 6. Demonstration of pixon-based denoising and deconvolution of time-resolved photoionization data for a transform-limited pump pulse. Partial success is seen in the lower trace; over resolution of the data occurs in the vicinity of 3 ps.

Figure 7. Raw data and hypothesis reconstruction for a pump pulse with the indicated positive chirp.

Figure 8. Raw data and hypothesis reconstruction for a pump pulse with the indicated negative chirp. The large peak during the second recurrence of the wave packet indicates wave packet focusing is obtained for this value of chirp.

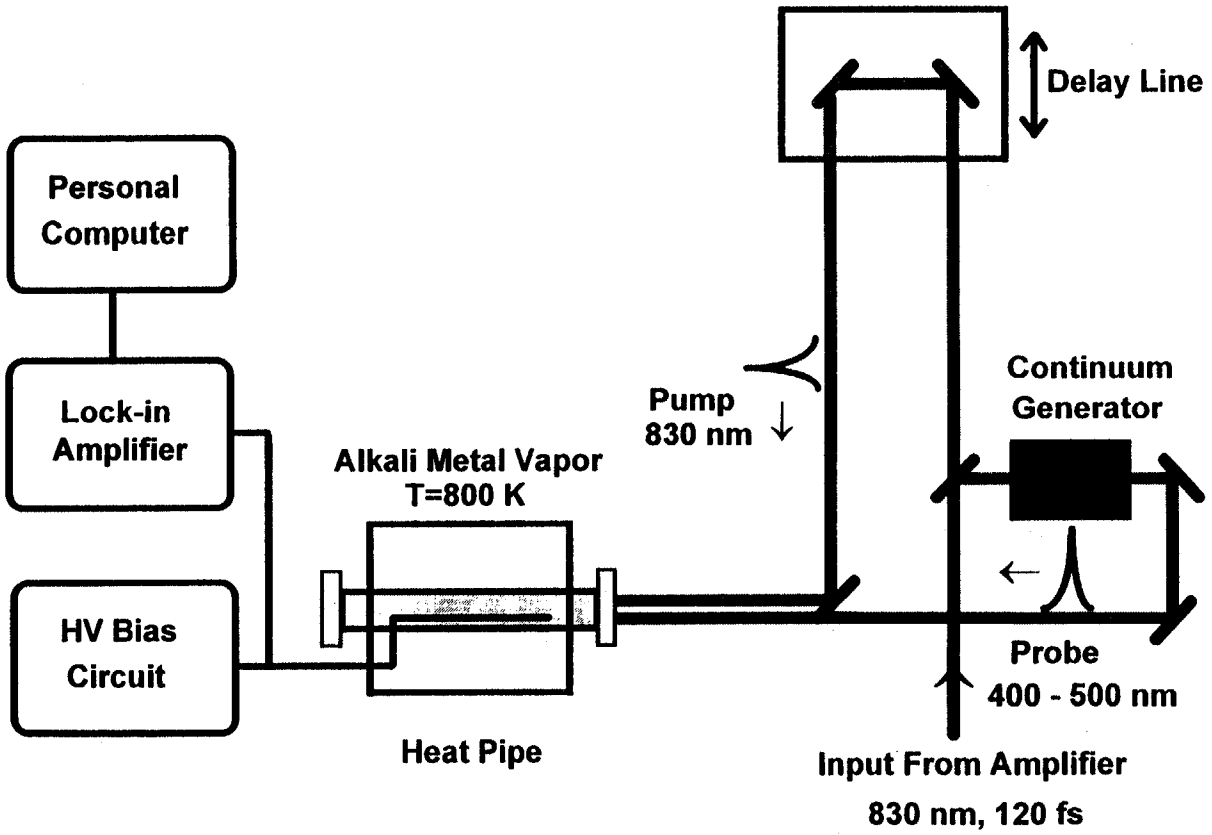
Delay Line
Personal Computer
Lock-in Amplifier
HV Bias Circuit
Alkali Metal Vapor
T=800 K
Pump
830 nm
Continuum Generator
Probe
400 - 500 nm
Heat Pipe
Input From Amplifier
830 nm, 120 fs

Figure 1

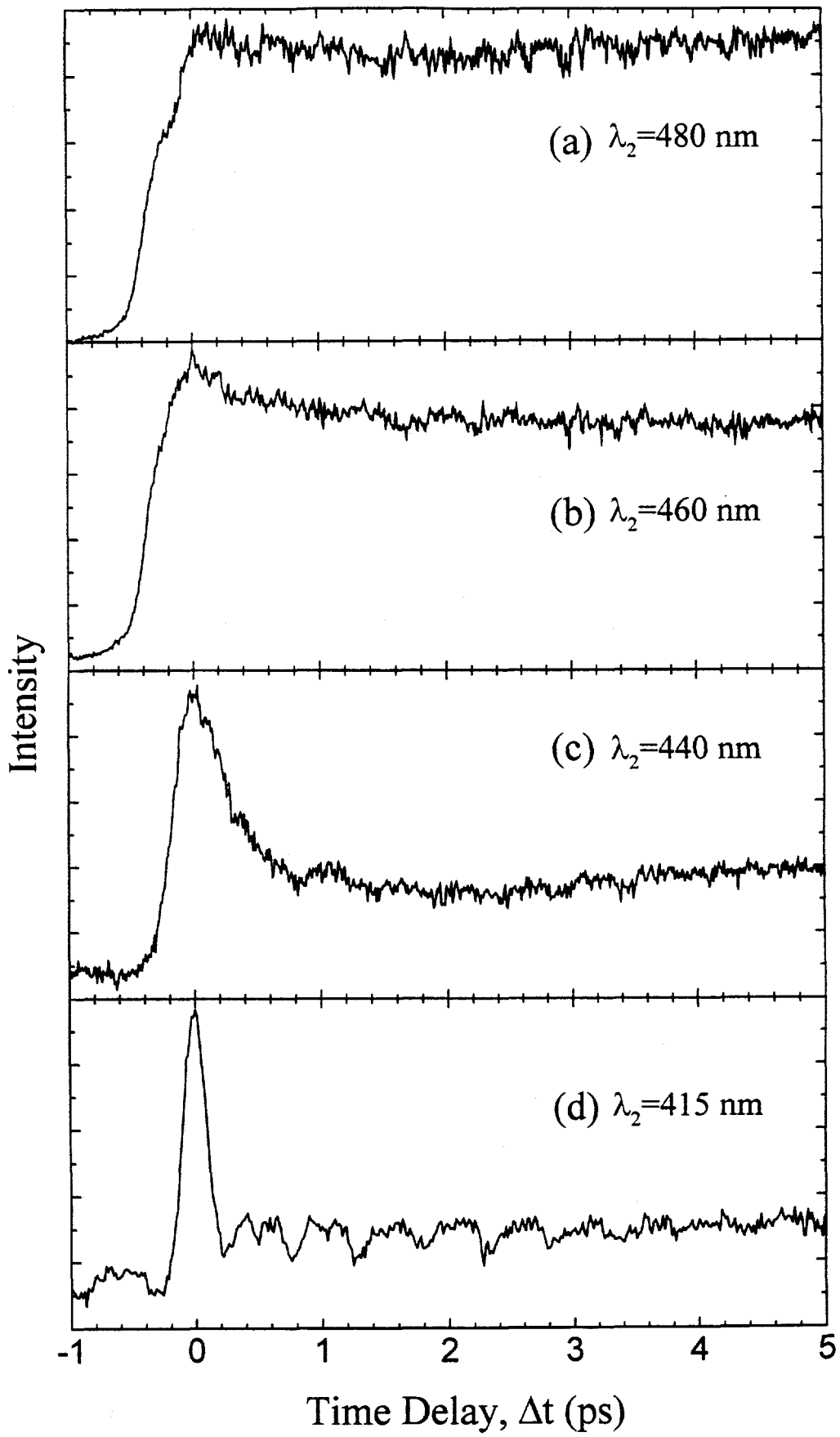
(a) λ2=480 nm
(b) λ2=460 nm
(c) λ2=440 nm
(d) λ2=415 nm
Intensity
-1
0
1
2
3
4
5
Time Delay, Δt (ps)

Figure 2

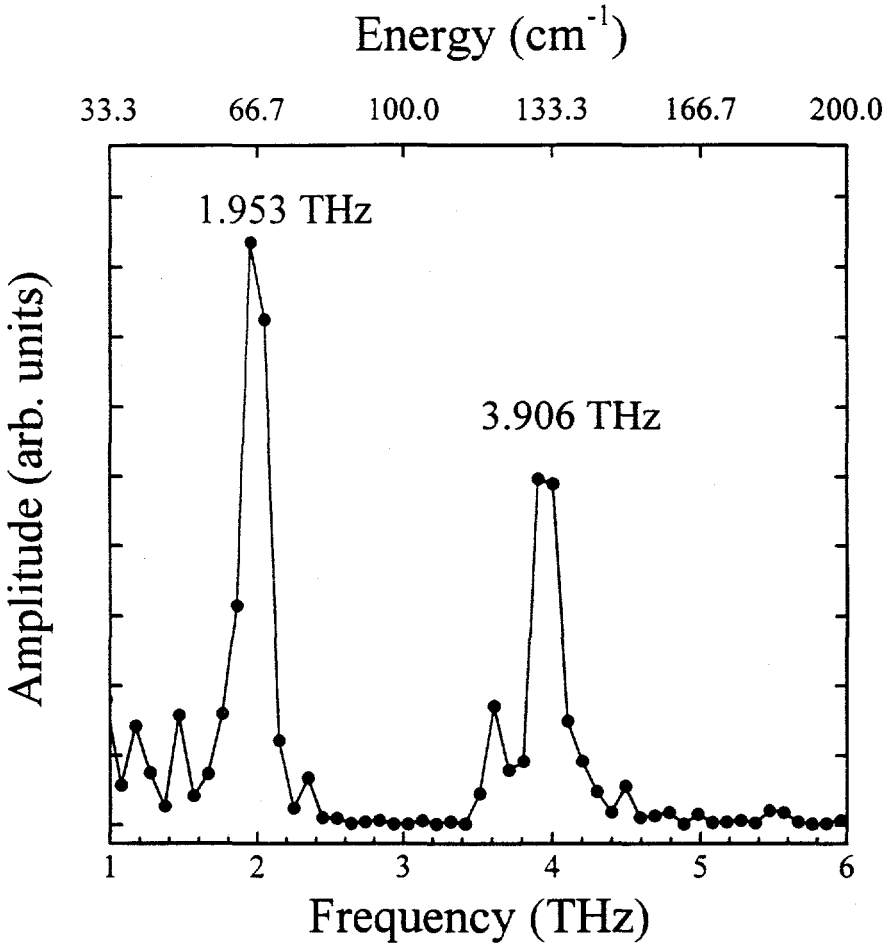
Energy (cm-1)
33.3
66.7
100.0
133.3
166.7
200.0
1.953 THz
3.906 THz
Amplitude (arb. units)
1
2
3
4
5
6
Frequency (THz)

Figure 3

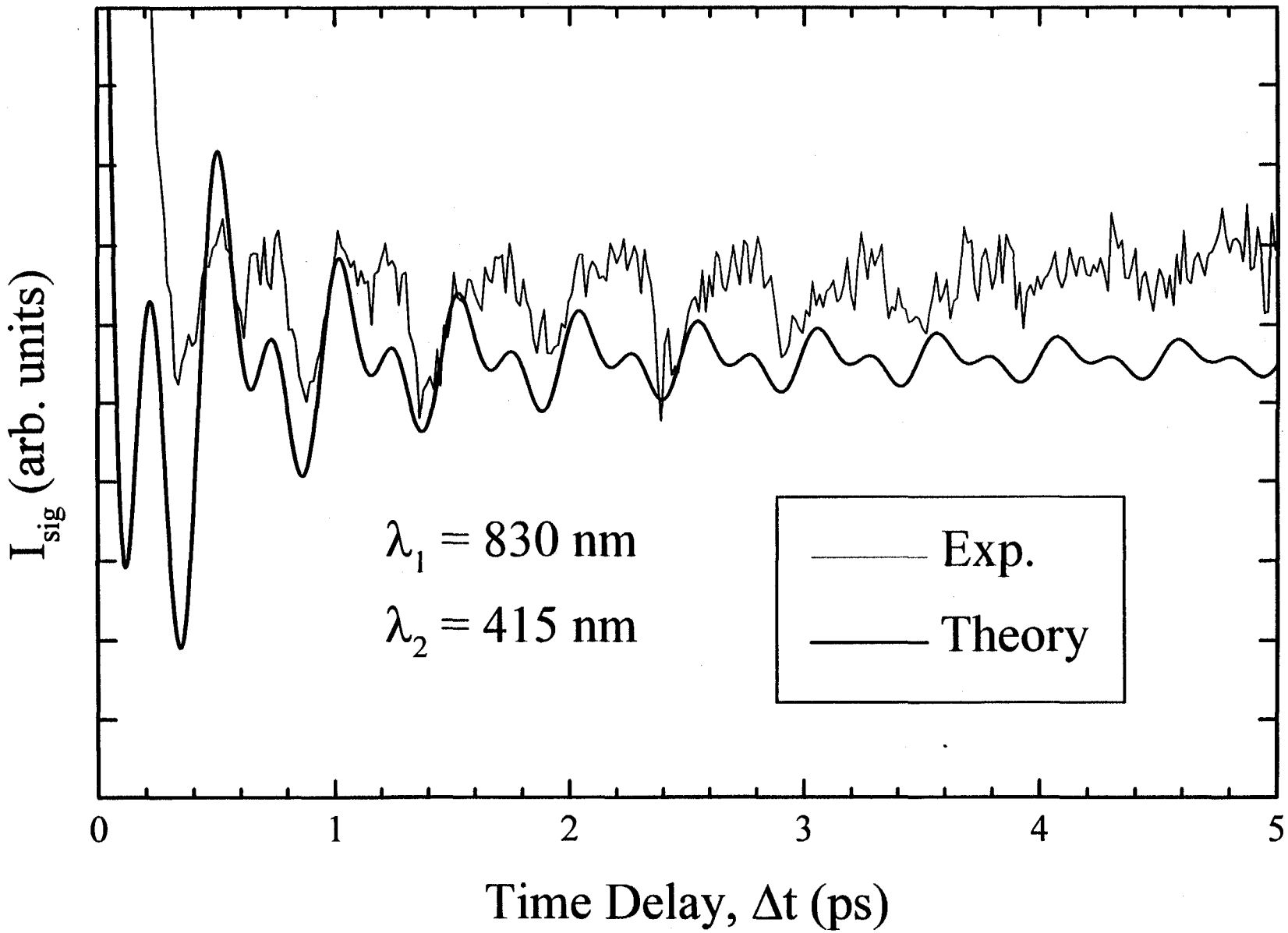
I_{sig} (arb. units)
$\lambda_1 = 830$ nm
$\lambda_2 = 415$ nm
Exp.
Theory
0
1
2
3
4
5
Time Delay, Δt (ps)

Figure 4

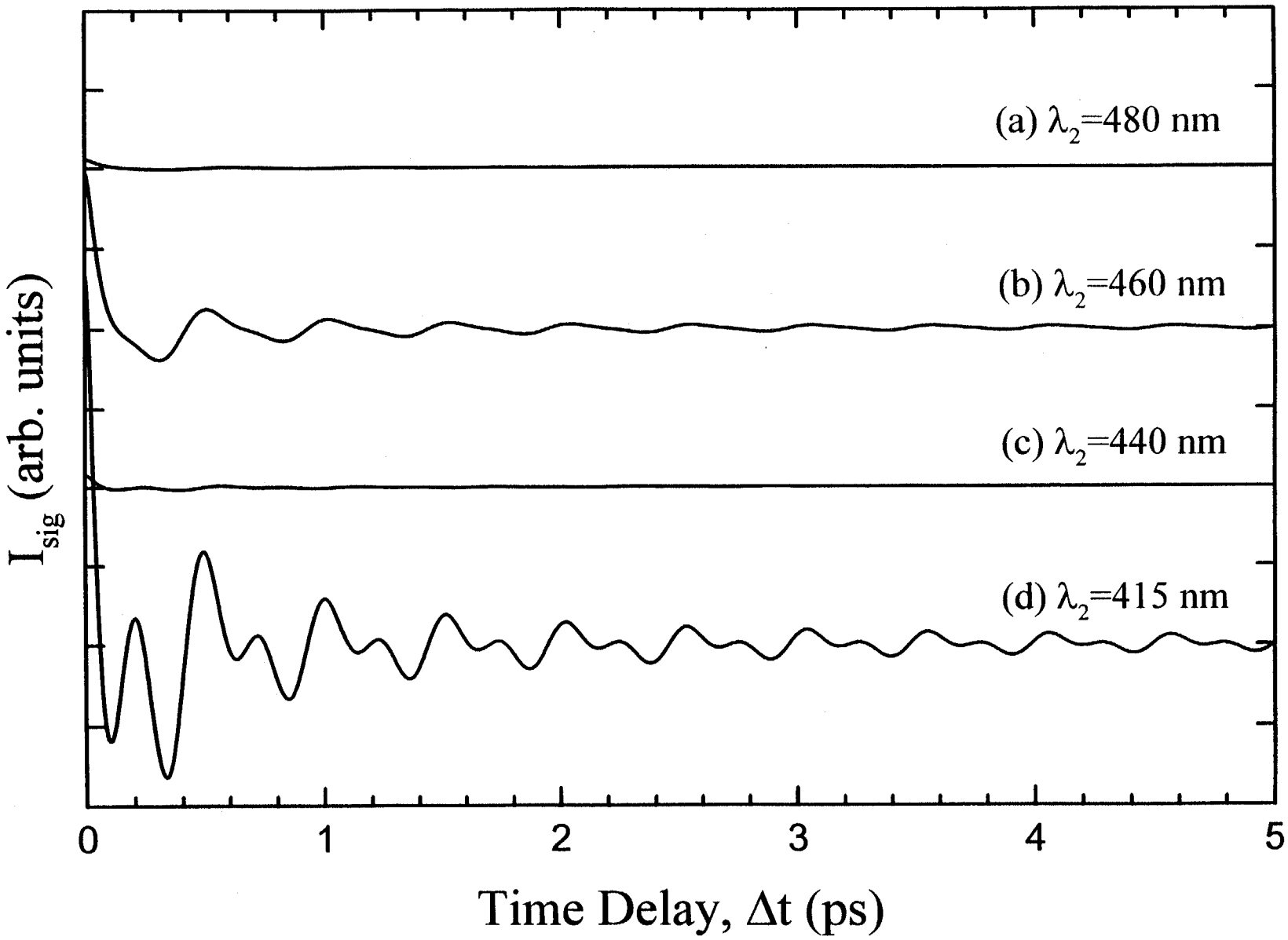
(a) λ2=480 nm
(b) λ2=460 nm
(c) λ2=440 nm
(d) λ2=415 nm
Isig (arb. units)
0
1
2
3
4
5
Time Delay, Δt (ps)

Figure 5

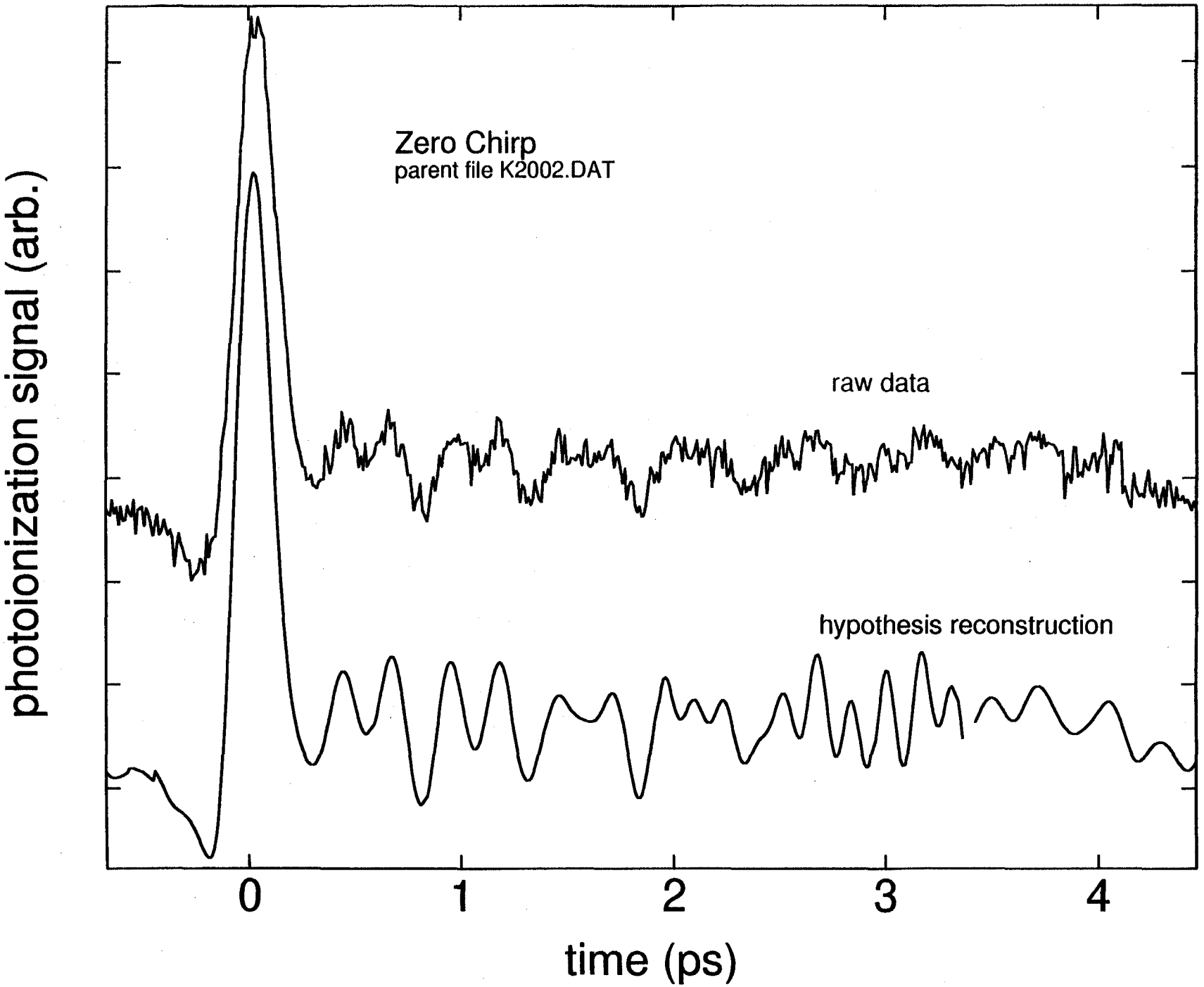
Zero Chirp
parent file K2002.DAT
raw data
hypothesis reconstruction
photoionization signal (arb.)
0
1
2
3
4
time (ps)

Figure 6

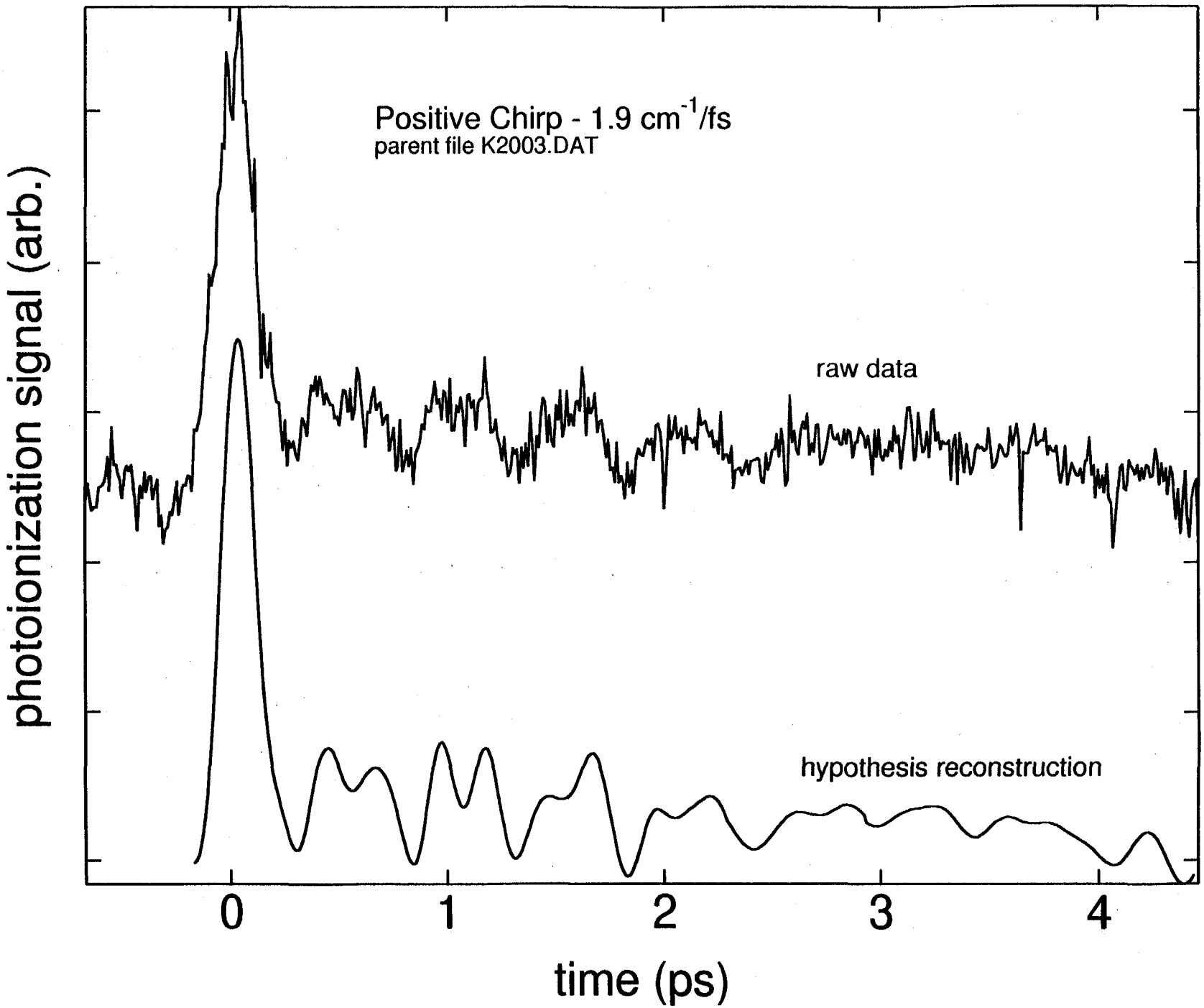
Positive Chirp - 1.9 cm^{-1}/fs
parent file K2003.DAT
raw data
hypothesis reconstruction
photoionization signal (arb.)
0
1
2
3
4
time (ps)

Figure 7

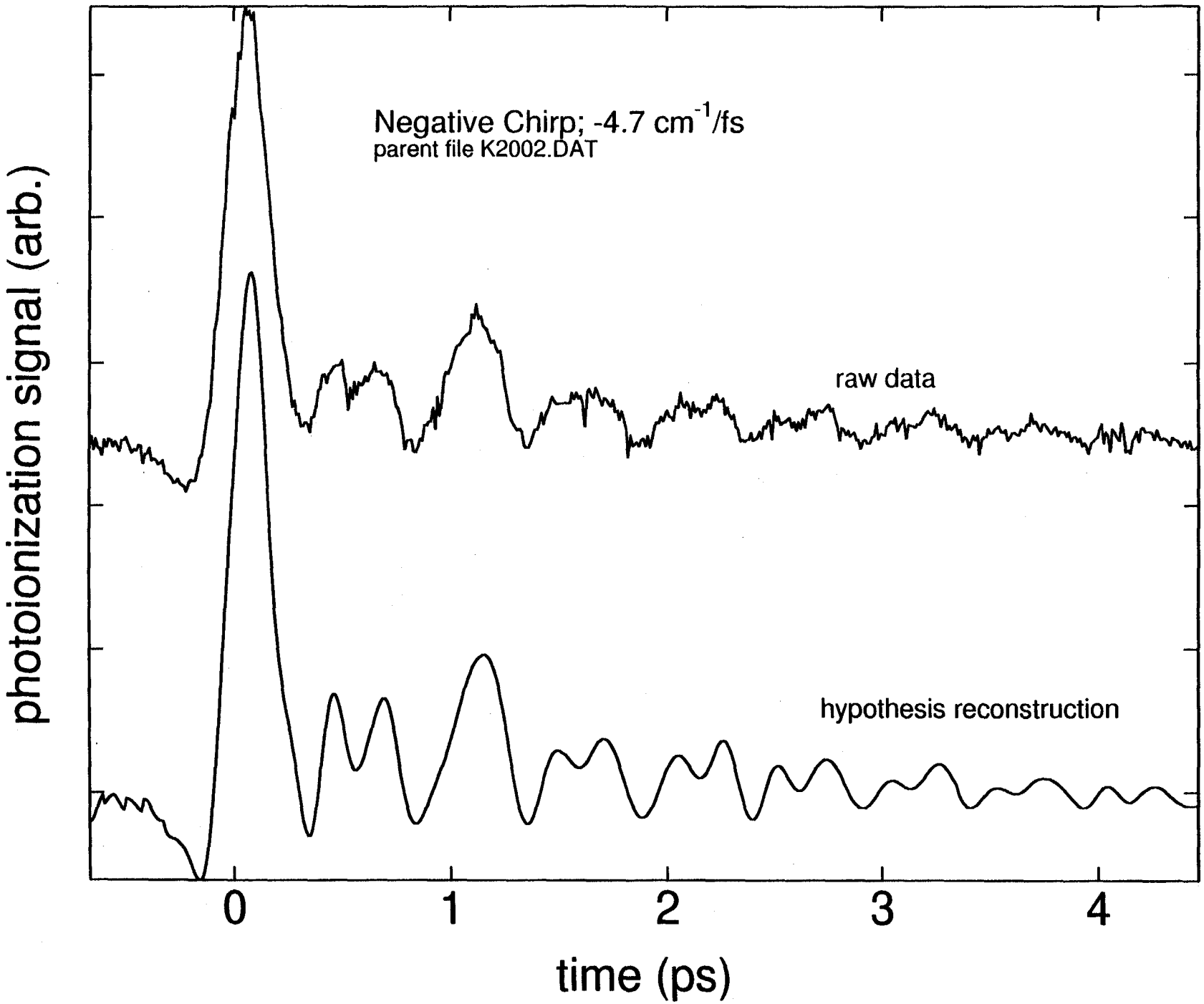
Negative Chirp; -4.7 cm^{-1}/fs
parent file K2002.DAT
raw data
hypothesis reconstruction
photoionization signal (arb.)
0
1
2
3
4
time (ps)

Figure 8